Friction scale effect in drilling natural fiber composites

Faissal Chegdani *, Mohamed El Mansori

Arts et Métiers ParisTech, MSMP Laboratory (EA7350), Rue Saint Dominique BP508, Châlons-en-Champagne, France

ARTICLE INFO

Keywords:
Natural fiber composites
Friction
Tool coating
Machining

ABSTRACT

This work aims to investigate the multiscale tribological behavior when drilling natural fiber composites by changing the tool-composite interface trough the modification of the tool coating. Drilling experiments were carried out on bidirectional flax fibers reinforced polypropylene resin using the same drilling tool geometry with three different coating properties. Results show that the tribo-mechanical behavior of the drilling operation is affected by changing the tool coating at different scale levels. This multiscale behavior is related to the intrinsic friction properties of each coating nature that influence the tribo-contact at the interface between the cutting tool edge and the composite surface.

1. Introduction

Manufacturing of natural fiber composites is among the real current industry challenges. This type of material offers both economic and ecological advantages in order to promote sustainable development by producing biodegradable and recyclable products [1–3]. The good processing of natural fiber composites implies the mastering of the different tribological aspects during manufacturing processes, especially when machining because cutting processes generate intimate friction contacts that can cause material damage and tool wear [4–7]. Understanding the friction produced by the tool geometry, the tool kinematic as well as the surface properties of the cutting tool seem to be important to control the tribological phenomena during machining operations.

Drilling of natural fiber composites has been investigated in few research works [8–13]. All these works have concluded that the feed rate and cutting speed are seen to contribute the most to the delamination effect. Generally, the use of high cutting speed and low feed leads to minimize delamination on drilling at hole extremities. However, considering high cutting speed and low feed in drilling natural fiber composites induces the maximum residual tensile strength which is not desirable for machining productivity and cutting edge sharpness [9]. Furthermore, it has been shown that the optimum drill point geometry for synthetic fiber composite laminates is not suitable for natural fiber-reinforced laminates because of the difference in the constituents and the material removal mechanisms [13].

Thus, drilling process of natural fiber composites needs more investigations to explore other parameters that can influence the machinability of these novel materials, especially the tribological parameters that control the tool/material contact. Indeed, the contact between the cutting tool and natural fiber composites is extremely complex due to the multiscale heterogeneous structure of natural fibers within the composite parts [14]. Therefore, the multiscale morphology of the tool surface must be considered when investigating the tribological phenomena in drilling natural fiber composites. The concept of intrinsic friction at cutting tool surface can hence be revealing. In fact, the surface intrinsic friction is the microscopic friction response that is only due to the microscopic morphology of this surface. The intrinsic friction is then a microscopic property of a given surface independently of any external contact or tribo-system interactions. Investigating the intrinsic friction of two surfaces can lead to understand the macro-tribological contact between these two surfaces as the friction is a multiscale concept [15]. Thus, the aim of this is to understand how this intrinsic friction can affect the macro-tribological contact when machining natural fiber composites.

In this paper, a particular focus will be placed on the tool/material contact tribology when drilling natural fiber composites regarding the cutting speed, the cutting feed and the tool coating by investigating three coating properties. Bidirectional woven flax fibers reinforced polypropylene resin will be considered for this study. Uncoated tungsten carbide, titanium diboride coated and diamond coated tools were used to conduct the drilling tests. Tribo-energetic approach will be adopted to evaluate the machinability at the considered cutting conditions. To understand the tribological drilling behavior regarding the tool coating properties, the intrinsic friction response of each coating type is determined with Atomic Force Microscope (AFM). Then, the induced machined surfaces are explored by Scanning Electronic Microscope (SEM) to show the functional relationship between the tribo-energetic

* Corresponding author.
E-mail address: faissal.chegdani@ensam.eu (F. Chegdani).

Fig. 1. a) Bidirectional woven flax fiber reinforcement. b) BDF/PP composite sheet.

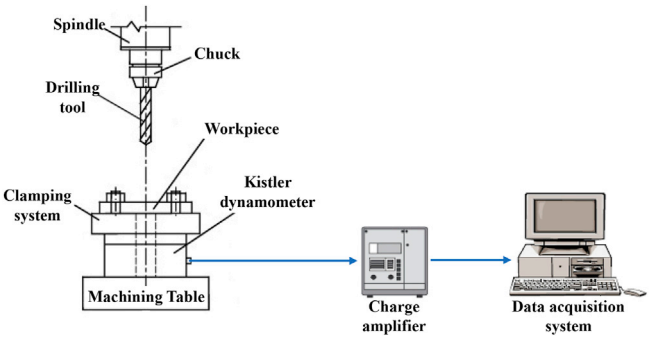

Fig. 4. Experimental drilling setup.

cutting behavior and the resulting surfaces state. Finally, the apparent drilling friction will be calculated using the in-situ measured cutting forces at each cutting configuration to show the frictional performances of the drilling operation on flax fiber composites.

2. Material and methods

2.1. Flax fiber composites

Flax fiber composites investigated in this study are composed of bidirectional woven flax fibers as shown in Fig. 1a. The used composites sheets (Fig. 1b) are bended by polypropylene matrix and are supplied by "Composites Evolution – UK". More technical data about the bidirectional flax fibers reinforced polypropylene composites (BDF/PP) are given in Ref. [6]. The BDF/PP workpieces have the total dimensions of 300 mm (length) × 35 mm (width) × 4 mm (thickness).

Table 1
Coating characteristics of each drilling tool.

	Uncoated	TiB2 coated	Dia. coated
Substrate	WC	WC	WC
Coating process	–	Monolayer PVD	Multilayer CVD
Coating composition	–	TiB_2	Diamond sp^3
Coating thickness (μm)	–	$2^{\pm 0.7}$	$7^{\pm 1}$
Measured edge radius (μm)	$5.5^{\pm 0.5}$	$8^{\pm 0.5}$	$11.5^{\pm 1}$

Table 2
Cutting conditions for drilling operations.

Tool coating	Feed rate (mm/min)	Cutting speed (m/min)
Uncoated	100	20
TiB2 Coated	200	30
Diamond Coated	300	40
		50
		60
		70

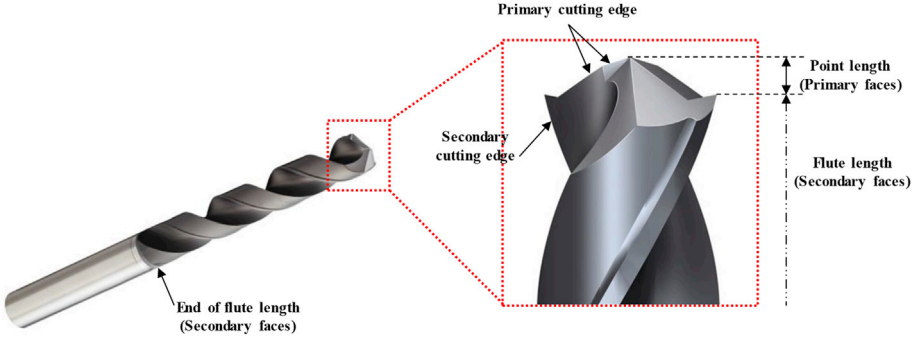

Fig. 2. Representative schema of the used drilling tool geometry (provided by Sandvik Coromant).

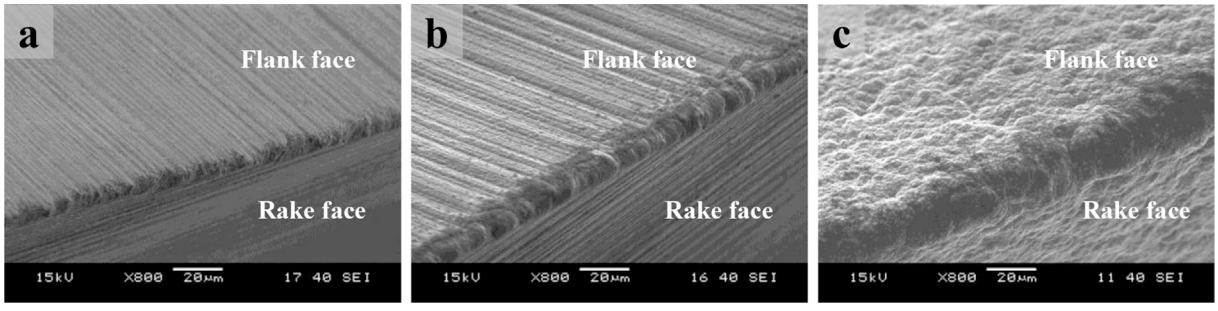

Fig. 3. SEM images of the primary cutting edge for each coated drilling tool: a) Uncoated, b) TiB2 coated and c) Diamond coated.

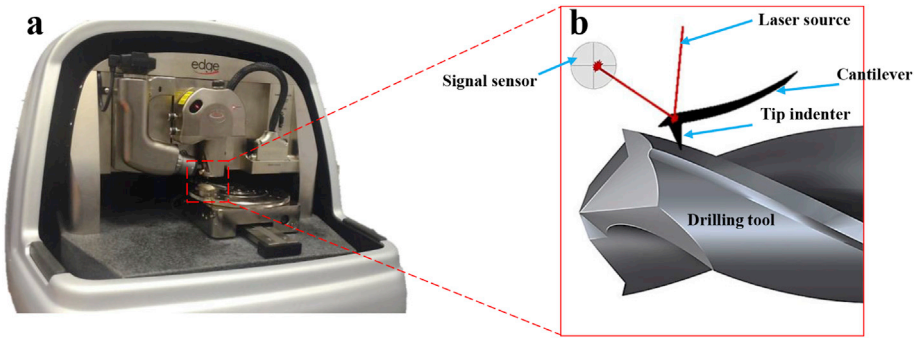

Fig. 5. Instrumented friction measurement on drilling tools by AFM.

Table 3
Sliding conditions for AFM friction measurements.

Applied load (μN)	Sliding speed (μm/s)
20	2
40	4
60	6
	8
	10

2.2. Coated cutting tools

Three iso-geometry helical carbide drill bits with 6 mm of diameter and composed of two cutting edges were provided by "Sandvik Coromant – FR" (Ref. 854.1-0600-05-A0) with different coating properties. The drilling tools have a point angle of 130°, a point length of 1.4 mm and a flute length of 42.6 mm. A representative schema of the used drilling tools is illustrated in Fig. 2. Uncoated tungsten carbide, monolayer physical vapor deposition (PVD) titanium diboride (TiB2) coated and multilayer chemical vapor deposition (CVD) diamond coated are considered. Changing the coating type doesn't affect the geometrical properties between the three studied drilling tools, except the tool-composite interface trough the change of the tool surface morphology and the cutting edge sharpness. Indeed, Fig. 3 shows that each coating type generates different surface morphology and different cutting edge radius. Diamond coating, which has the highest thickness, generates the highest cutting edge radius as shown in Table 1. More technical data about CVD and PVD processes are given in Ref. [5].

2.3. Drilling operations

Drilling experiments were performed on instrumented three axes CNC machine as described in Fig. 4. Experimental system was mounted on a Kistler dynamometer (model 9271A) in order to measure the drilling thrust and torque. The acquired drilling signals were converted into voltage signals using a multichannel charge amplifier (type 5019A130). Data acquisition system was performed with a data acquisition device (National Instruments, USA), along with a data recorder (LabVIEW software) at 1000 Hz sampling rate.

Tests have been conducted on dry cutting contact conditions at different cutting speeds and feed rates. All other cutting parameters were kept constant. The drilling process parameters are presented in Table 2. In order to get reliable results, each test was repeated three times under identical conditions and with a new cutting tool at each time. Thus, the output values from drilling experiments are presented as the mean of these three repeated tests. Errors are considered as the average of the absolute deviations of data repeatability tests from their mean.

2.4. AFM friction measurements

Friction measurements on coated cutting tool were performed by

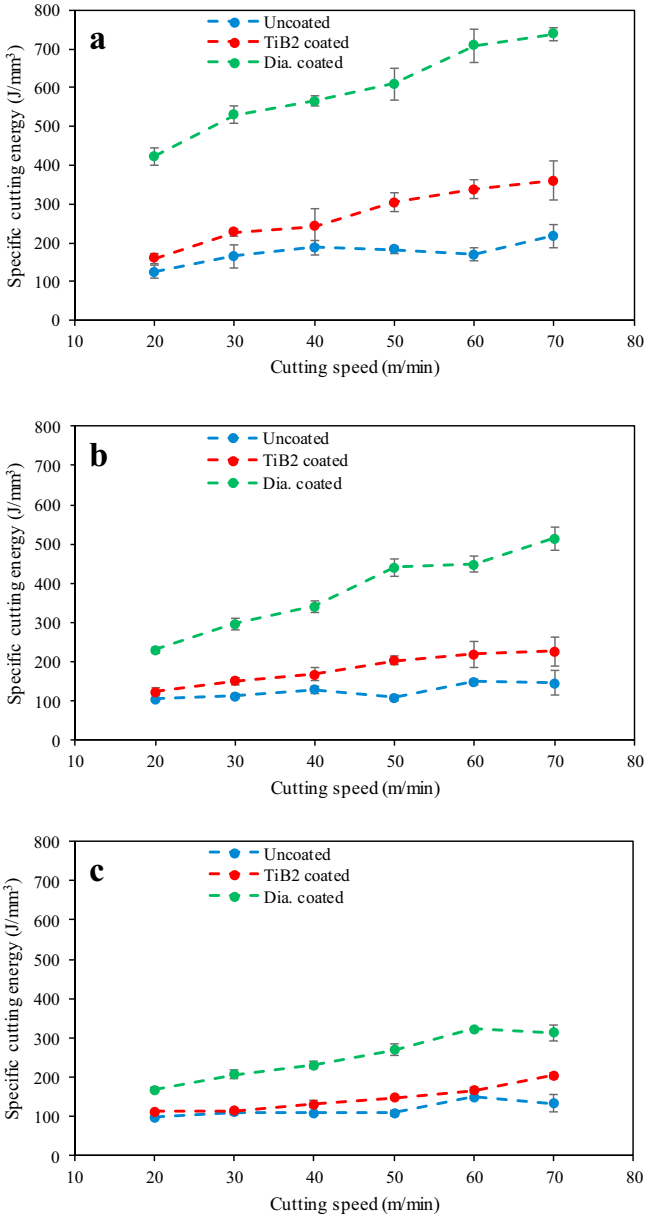

Fig. 6. Specific cutting energy for the three considered coated drill tools at the different drilling conditions. a) at V_f = 100 mm/min, b) at V_f = 200 mm/min, c) at V_f = 300 mm/min.

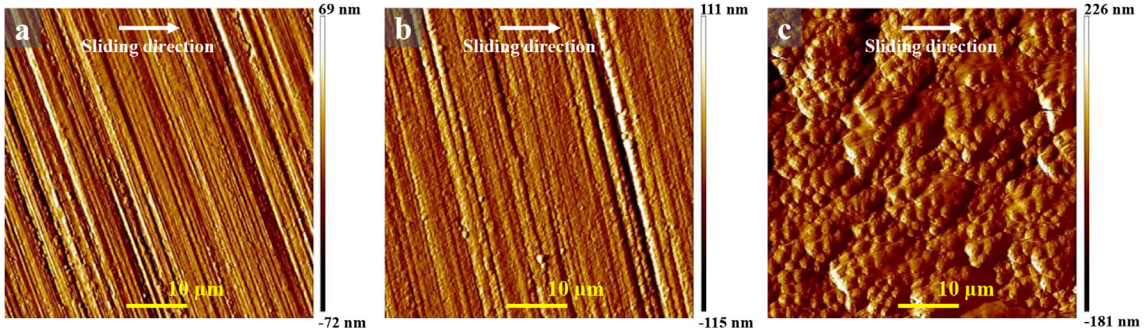

Fig. 7. AFM scan images of the three considered coated tools. a) Uncoated tool, b) TiB2 coated tool, c) Diamond coated tool.

atomic force microscopy "*Dimension Edge*™ - *Bruker*" as shown in Fig. 5. AFM instrument has been used with a Berkovich diamond tip indenter with small tip radius (~40 nm). The tip indenter is related to a steel cantilever that has a spring constant of 450 N/m. The tip indenter slides on the tool-coated work surface at constant load and sliding speed in the flank face of the secondary cutting edge which is easier to set up as shown in Fig. 5b. Since the coating is uniformly deposited on the drilling tool, the measurement of the friction response on the secondary cutting edge will reveal the intrinsic friction signature of each coating interface. The considered sliding distance is 10 µm in order to work near to the active zone (i.e. near to the cutting edge). The friction signal is measured over the sliding distance and the friction coefficient is determined by computing the ratio between the mean friction signal and the applied load at each sliding condition. Table 3 presents the studied sliding conditions.

3. Results and discussion

3.1. Energetic analysis of drilling

The energetic analysis consists on determining the specific cutting energy (E_c (N.mm^{-2})) that can be calculated by equation (1) where M_c (N.mm) is the measured drilling torque, ω (rad.min^{-1}) is the angular velocity and Q (mm^3.min^{-1}) is the material removal rate.

$$E_c = \frac{M_c \times \omega}{Q} \quad (1)$$

The angular velocity can be determined from the cutting speed (V_c (m.min^{-1})) and the drill diameter (D (mm)) by the equation (2). The material removal rate is calculated using equation (3) where V_f (mm.min^{-1}) is the feed rate.

$$\omega = \frac{2000 \times V_c}{D} \quad (2)$$

$$Q = \frac{\pi \times D^2 \times V_f}{4} \quad (3)$$

Fig. 6 presents the results of specific cutting energy at all the drilling conditions. The specific cutting energy of the three drill tools increases by cutting speed increasing and decreases by feed rate increasing. There is a slight difference between the uncoated tool and the TiB2 coated tool, especially when increasing the feed rate. At high feed rate, the effect of cutting speed becomes less significant. Furthermore, specific cutting energy increases significantly when using the diamond coated drill tool. In addition, the effect of tool kinematic is more obvious by the diamond coated tool. However, it tends to behave in similar way as the other coated tools at high feed rate. Since the specific cutting energy is an indicator of material machinability [16], it can be concluded that diamond coated tool deteriorates the machinability while the uncoated tool improves it.

The specific cutting energy in Fig. 6 is a global concept. It contains different tribological mechanisms that occur during the drilling operation. Typically, the specific cutting energy (E_c) can be considered as a

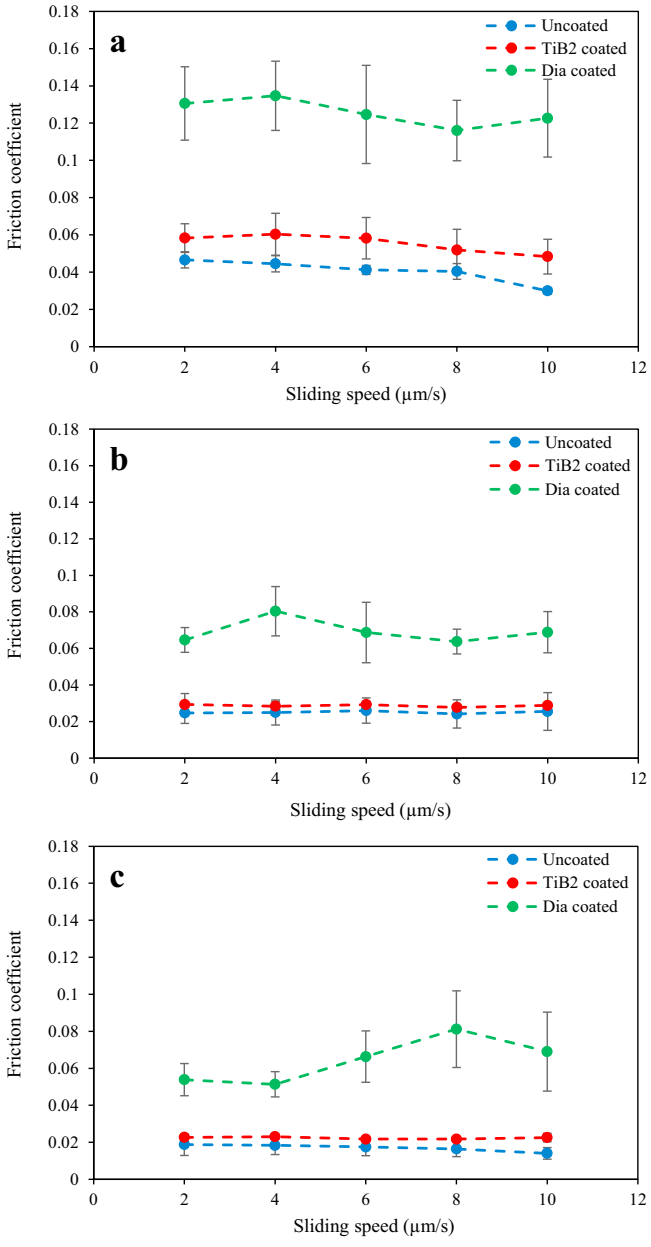

Fig. 8. AFM friction response of the three considered coated drill tools at different applied loads: a) at 20 µN, b) at 40 µN, c) at 60 µN.

combination of three principal components: the shearing energy ($E_{shearing}$), the deformation energy ($E_{deformation}$) expended by the deformation when drilling, and the friction energy ($E_{friction}$) dissipated by sliding friction [4,17] following the equation (4).

$$E_c = E_{shearing} + E_{deformation} + E_{friction} \quad (4)$$

By considering these three physical mechanisms, the energetic behavior of the drilling operation regarding the tool coating can be explained. Indeed, adding a coating to a cutting tool increases the cutting edge radius as shown in Fig. 3. Diamond coating generates the highest cutting edge radius because of its high thickness as shown in section 2.2. Consequently, increasing the cutting edge radius favors the fibers deformation inside the composite structure before being sheared by increasing the cutting contact area as previously demonstrated for the milling process [5]. This will increase the deformation component ($E_{deformation}$) of the specific cutting energy as well as the shearing component ($E_{shearing}$) since the fiber shearing becomes difficult by increasing the cutting edge radius [5].

On another side, the sliding friction component ($E_{friction}$) is dependent of the surface properties of the two materials in contact. Changing the tool coating type changes the tool surface morphology and then the tool/material contact property. It's interesting to investigate the intrinsic tribological signature of each tool coating for more understanding of the sliding friction behavior when drilling. This is the aim of the next section.

3.2. Intrinsic sliding friction signature of coated tools

To reveal the difference in the intrinsic friction signature of each coated tool, it is necessary to work at microscopic scales that present the scales of surface morphology changes regarding the tool coating type (Fig. 3). AFM instrument has been used in contact mode for friction tests on coated tools [14]. The considered zone for the indentations (50 μm × 50 μm) has been scanned near to the cutting edge by the same AFM mode to well target the tip indenter position and the sliding distance. Fig. 7 shows the scan images of the tool surfaces that correspond to the deflection signal of the indenter. These scan images reveal the morphological difference between the three cutting tools according to the considered coating type as previously observed in the SEM images of Fig. 3. The mean arithmetic roughness (R_a) in the scan area is 15 nm for uncoated tool, 20 nm for the TiB2 coated tool and 44.9 nm for the diamond-coated tool. Each sliding test is repeated six times at different places of the scan area in the same conditions to verify the repeatability. As for the cutting forces (section 2.3), the intrinsic friction coefficient (described in section 2.4) is presented as the mean of these six repeated

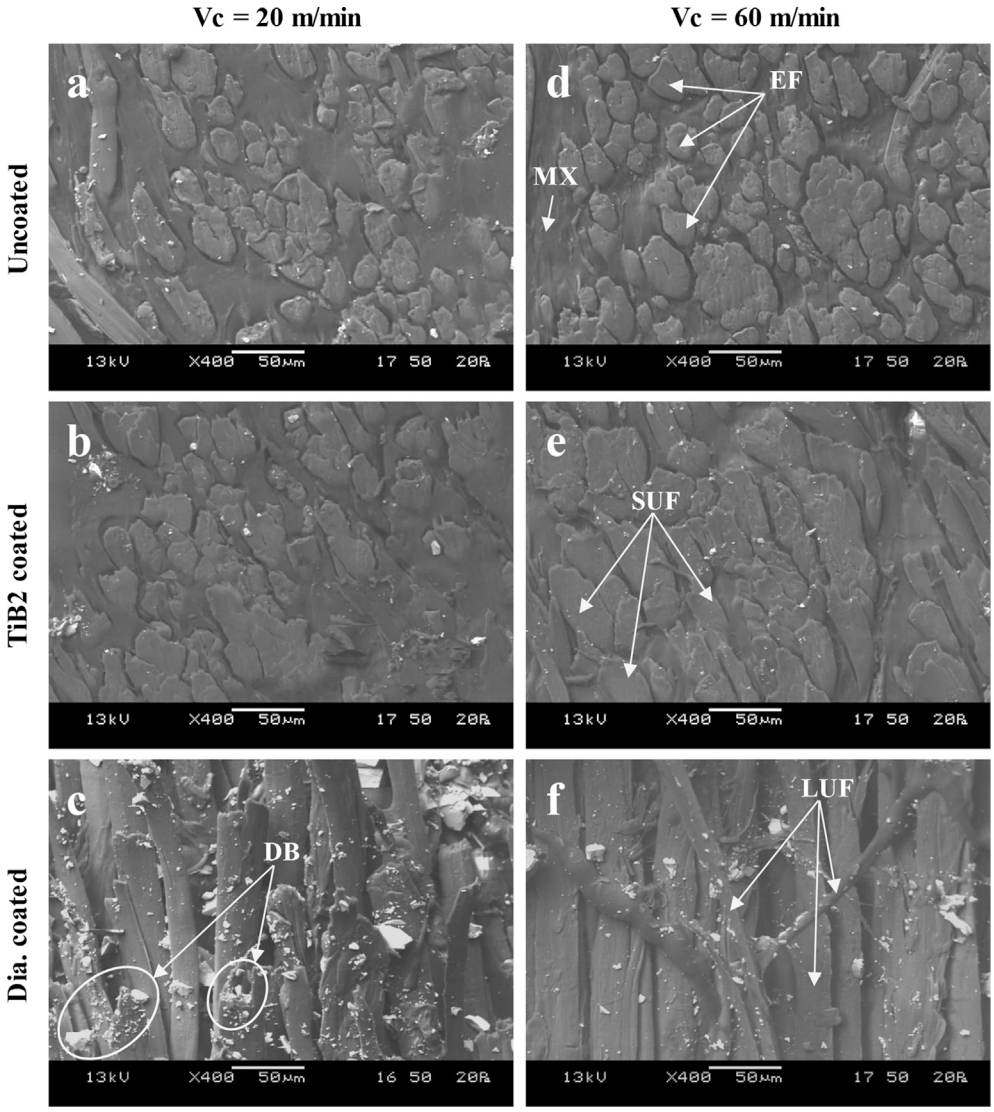

Fig. 9. SEM images of the machined lateral surfaces drilled by the three considered tools with feed rate $V_f = 100$ mm/min. EF: Elementary fibers, MX: Matrix, DB: Debris, SUF: Short uncut fibers, LUF: Long uncut fibers.

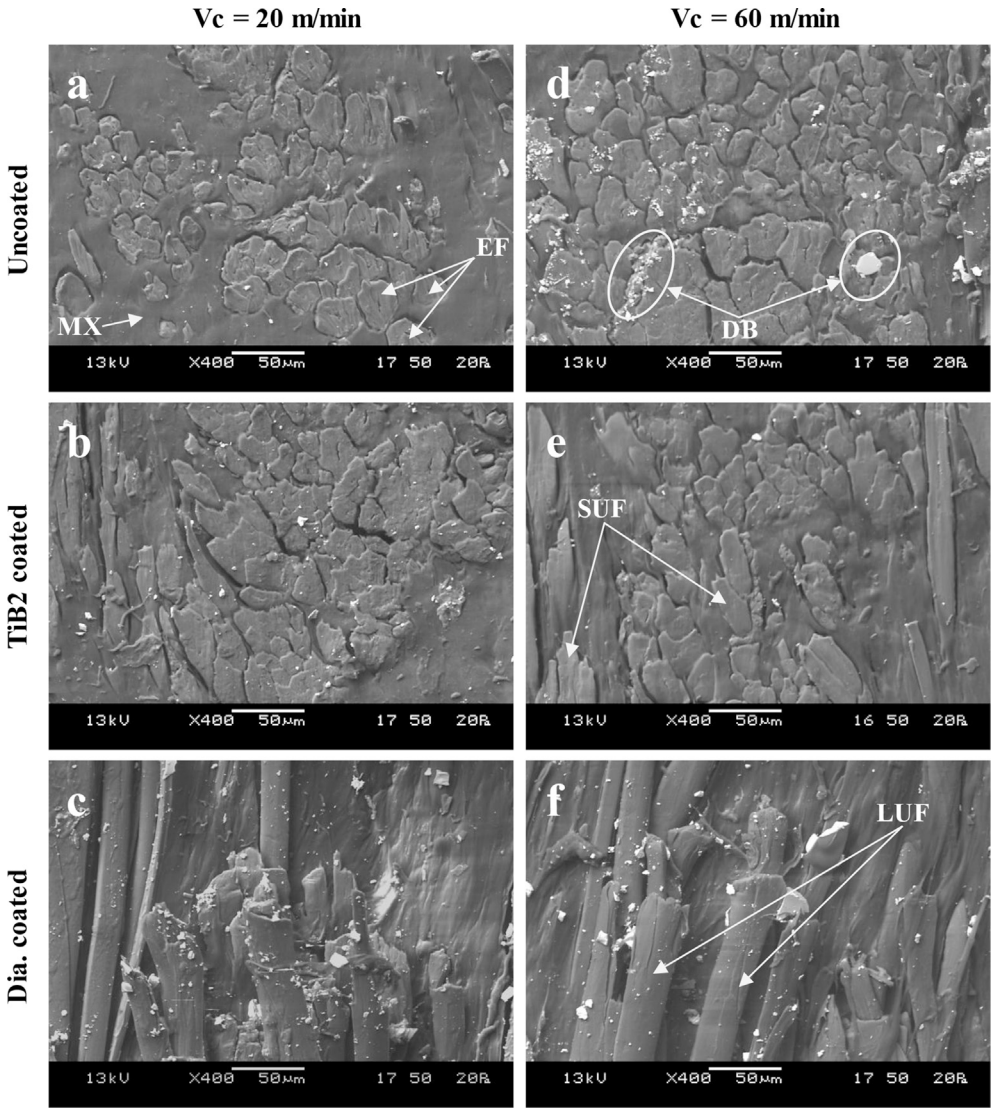

Fig. 10. SEM images of the machined lateral surfaces drilled by the three considered tools with feed rate V_f = 300 mm/min. EF: Elementary fibers, MX: Matrix, DB: Debris, SUF: Short uncut fibers, LUF: Long uncut fibers.

tests. Errors are considered as the average of the absolute deviations of data repeatability tests from their mean.

It's important to notice that the objective here is not to quantify the sliding friction contribution in the cutting energy of the last (section 3.1) because the process is not the same and the tool/tip indenter contact cannot be compared to the tool/composite contact. The aim of this section is to determine whether the tool coating type influences the intrinsic friction signature of the cutting tools at micro-scale. This will allow more understanding of how the sliding friction can behave by changing the tool coating property when drilling.

Fig. 8 presents the intrinsic friction behavior of the considered cutting tools in function of sliding speed for different applied loads. Globally, the sliding speed effect at these micro-sliding scales is insignificant and the applied load contributes to reduce the friction response. Uncoated tool and TiB2 coated tool seems to behave in the same way when increasing the applied load. Diamond coated tool generates the highest friction response which is about more than the double of the friction values generated by the other cutting tools.

At micro-scale, diamond coating presents the roughest surface with a high density of surface asperities (Fig. 7c). TiB2 coating generates a surface topography which suits that of the tungsten carbide substrate. However, TiB2 coating induces more surface asperities than the uncoated surface substrate as shown in Fig. 7a and b. Thus, the difference of the surface topography between the three cutting tools at micro-scale will affect the real contact surface which controls the intrinsic friction response of each coated cutting tool.

Fig. 8 shows that the intrinsic friction responses of the cutting tools behave in the same way as their own specific drilling energies in Fig. 6. This is the sign that the micro-friction properties of the tool coating can influence the machinability when drilling flax fiber composites by affecting the tribological phenomena at the interface between the tool surface and the composite surface. The machinability of flax fiber composites at different drilling conditions will be evaluated in the next section.

3.3. *Micrographs of the machined surfaces*

Microscopic observations of surface state were made by scanning electron microscope (SEM/model JSM-5510LV) at low vacuum mode (20 Pa) without any coating of the samples. Typical representative surface morphologies as induced by drilling at the lateral surfaces of the drilling holes are hence presented in this section. To target the desired lateral surfaces, the drilling holes were cut from their centers by water jet cutting.

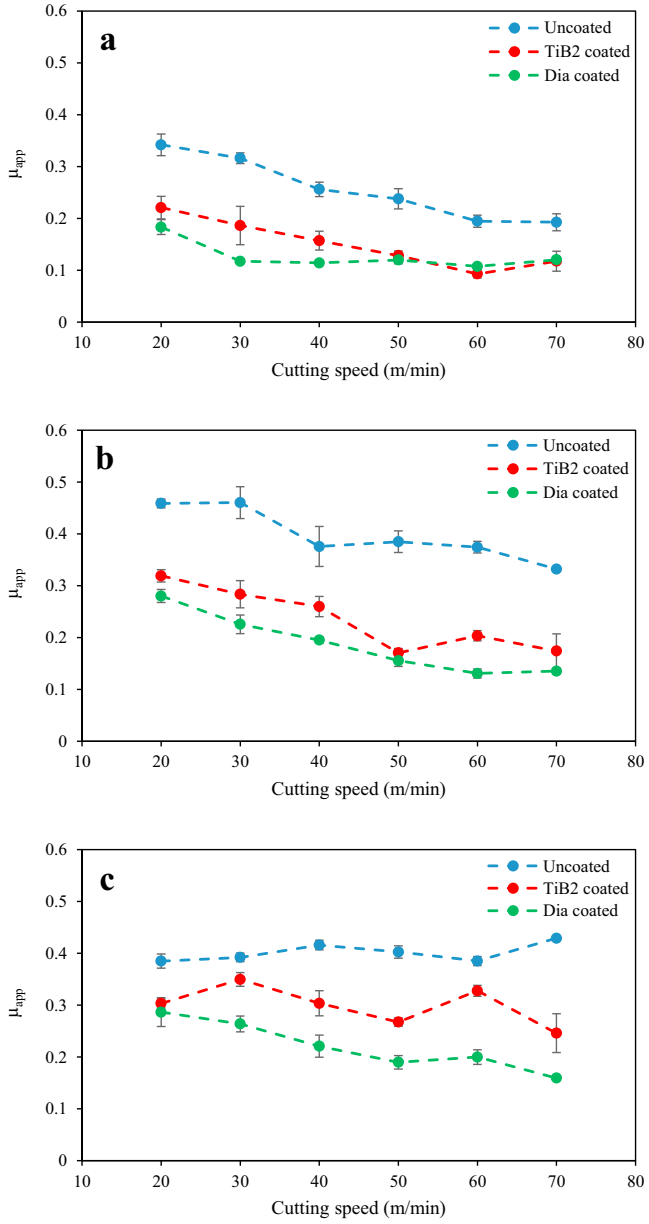

Fig. 11. Apparent drilling friction for the three considered coated drill tools at the different drilling conditions. a) at V_f = 100 mm/min, b) at V_f = 200 mm/min, c) at V_f = 300 mm/min.

Figs. 9 and 10 show the microscopic machined surfaces state for the three considered cutting tool at different cutting conditions. The microscopic observations are in total consistency with the energetic analysis carried out in section 3.1. Indeed, the uncoated cutting tool offers the best machinability, especially at high feed rate. Thus, the elementary flax fibers are well cut as we can observe the cross section of the fibers (Fig. 10a,d). It can be notice that the effect of cutting speed is insignificant at high feed rate. Machinability in the case of TiB2 coated tool is acceptable at high feed rate and low cutting speed, However, it can be seen some uncut fiber extremities due to fiber deformation and, then, the fibers cross section is not clearly visible. Moreover, the diamond-coated tool presents the poorest machinability at all cutting conditions. The fibers are strongly deformed and remain on the machined surface without being cut (Fig. 9c,f). The fibers are not cut but torn-off (Fig. 10c,f). This inevitably explains the very high specific cutting energy produced by diamond-coated tools.

The SEM observations of this section show that the considered cutting

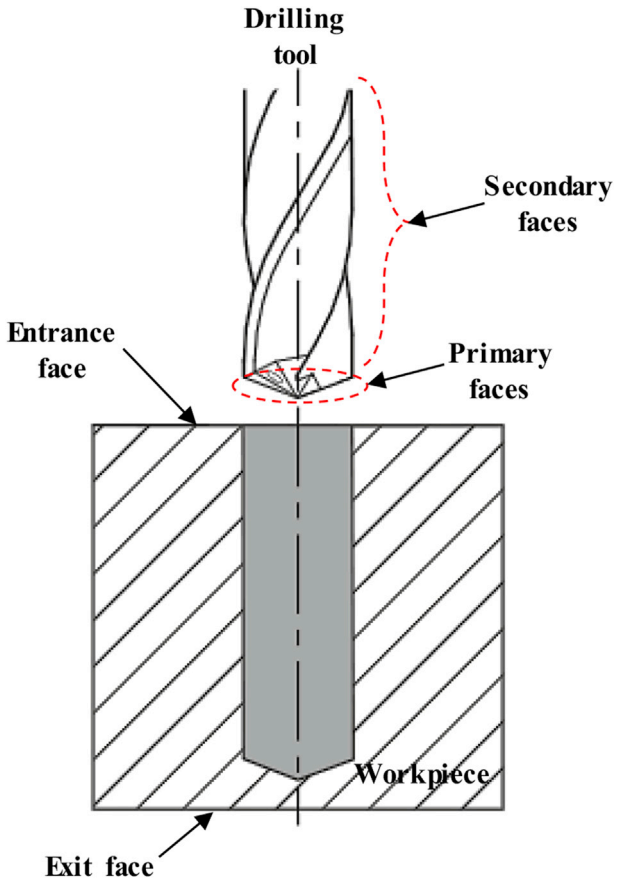

Fig. 12. Schematic diagram of drilling tool operation.

conditions change the machined surface characteristics by affecting the rate of the uncut flax fibers on the machined surfaces. This will influence the tribological properties during the drilling operation, especially the drilling friction between the tool and the composite. The next section will investigate these tribological phenomenon.

3.4. Multiscale drilling friction behavior

Macroscopic drilling friction is inspected using the in-situ apparent friction coefficient (μ_{app}) which involves different friction contacts: sliding contact between rake tool face and removed chip surface, sliding contact between flank tool face and machined surface, in addition to the contact between the secondary flank surface and the machined surface. μ_{app} can be obtained by the equation (5) where M_c (N.mm) is the drilling torque, F (N) is the drilling thrust and R (mm) is the drill radius [18].

$$\mu_{app} = \frac{M_c}{F \times R} \tag{5}$$

Fig. 11 shows the drilling friction behavior for all the cutting conditions. Uncoated drilling tool induces more friction comparing to the other coated tools. The induced friction difference between TiB2 coated tool and diamond coated tool is more obvious at high feed rate where TiB2 coated tool generates more friction than diamond coated tool. The cutting speed reduces the friction except at high feed rate where its effect becomes insignificant.

It can be seen that the microscopic intrinsic friction response induced by tool coating (section 3.2) influences the macroscopic drilling friction response by changing the cutting edge surface morphology and the cutting edge radius. However, diamond coating, which have the highest intrinsic friction response, induces the lowest apparent drilling friction.

Friction is a complex phenomenon that cannot be reduced to a single

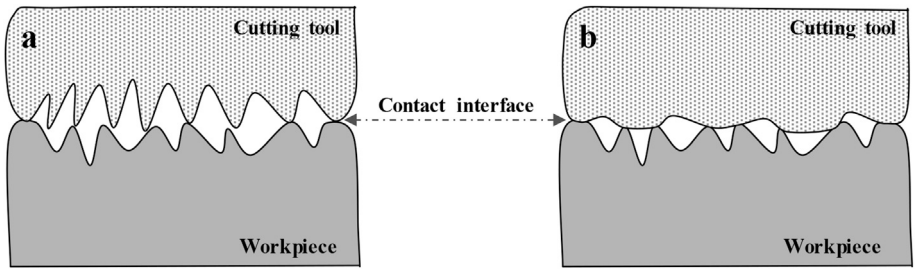

Fig. 13. Schematic depiction of the real contact area between the cutting tool surface and the composite surface at microscale. a) High tool surface roughness. b) Low tool surface roughness.

mechanism. But rather is a result of simultaneous action of various mechanisms at different scale levels [15]. In the case of drilling, the friction is more complex because the apparent friction considers the contact between the composite material and different surfaces of the cutting tool such as the primary and the secondary rake faces, the primary and the secondary flank faces, the primary edge radius area, and the secondary edge radius area. The friction forces differ for each tool side/material contact at each step of drilling operation. Indeed, the contact between the composite material and the primary cutting edge, primary rake face and primary flank face will be at the cutting step when the drilling tool crosses the workpiece from the entrance face to the exit face of the material (Fig. 12). At this drilling step, the specific energy is the highest because the material shearing occurred and controls the dissipative energy behavior. The shearing mechanism is revealed at mesoscale when the contact is arisen between the primary cutting edge and the composite material, especially the flax fibrous structure that is composed of flax fiber bundles (between 50 μm and 100 μm of diameter). At this contact scale, the cutting edge radius value has a significant effect and controls the cutting process. Consequently, the diamond coating, that has the highest cutting edge radius, induces the highest drilling energy since the shearing mechanism at this scale becomes difficult by increasing the cutting edge radius.

Since the point length exceeds the exit side of the material, no contact is occurred with the primary faces and the drilling operation is reduced to the sliding friction:

- between the lateral machined surface of the drilled holes and the secondary flank face of the drilling tool.
- Between the removed chip and the secondary rake face of the drilling tool.

These two sliding friction processes controls the apparent drilling friction at macroscale. To understand why the drilling friction induced by diamond coating tool is the lowest when drilling flax fiber composites even if the intrinsic friction response of diamond coating is the highest, it's necessary to investigate the friction mechanisms on microscale of the surface asperities.

At the asperities scale, two main mechanisms can occur: adhesive friction and deformation of asperities. Both friction mechanisms are directly proportional to the real contact area and, thus, the friction force increases by increasing the real contact area [19,20]. However, every nominally flat surface has a roughness and the real contact area is only a small fraction of the nominal contact area because the contacts take place only at the summits of the asperities [15] as described in Fig. 13. Considering the high difference of hardness between the tool surface material and the flax composite material [5], only the composite surface material will be affected by adhesion and deformation mechanisms. Therefore, the more the tool edge surface has asperities the more the real contact area decreases and, then, the micro-friction induced by adhesion and deformation decreases. Consequently, the diamond coating, that have the highest roughness, induces the lowest drilling friction from a microscopic point of view.

At mesoscopic scale, an additional mechanism must be considered. Mesoscale is the pertinent scale for machining analysis and corresponds to the flax fibrous structure size. As shown in section 3.1 and SEM images of section 3.3, using diamond coating tool induces a high rate of uncut fiber extremities that exceed the lateral machined surface of the drilled holes. Therefore, the friction contact at mesoscale will be not only with the PP matrix and the cross sections of elementary fibers, but also with these uncut fiber extremities that play a role of third body and affect the tool/material contact interface. A third-body mechanism is then occurred at mesoscale and tends to reduce the friction at this scale since flax fibers plays a role of third body lubricant as explained in Ref. [6]. Consequently, the diamond coating, that generates the highest uncut fiber extremities, induces the lowest drilling friction from a mesoscopic point of view.

To summarize, this work shows the scale effect on the tribological behavior in drilling flax fiber composites. The overall macroscopic behavior is influenced by multiscale phenomena that arise at micro- or meso-scales. This is the specificity of natural fiber composites that have multiscale tribo-mechanical behavior as demonstrated by a previous work of the authors [14]. It can be seen the shearing and third-body mechanisms are revealed at the meso-scale (i.e. scale of the flax fibers bundle), while the adhesion and deformation mechanisms are affected at the micro-scale that is the scale of the surface morphology changes of the faces in contact when drilling. Even if the intrinsic friction response of diamond coating is the highest, the drilling friction induced by diamond coating tool is the lowest when drilling flax fiber composites. This macro-friction behavior is due to the different friction mechanisms that occur at two different scale levels (micro and meso).

4. Conclusions

This paper is focused on the multiscale tribological influence of tool coatings on the machinability of bidirectional woven flax fiber reinforced polypropylene composites. For this aim, uncoated tungsten carbide, titanium diboride coated and diamond coated tools were used to conduct the drilling tests by varying the tool kinematics. The following conclusions can be drawn:

- Introducing a tool coating damages the machinability of flax composites by increasing the specific cutting energy during drilling operation. Increasing the cutting speed increases the cutting energy while increasing the feed rate decreases the cutting energy and reduces the cutting speed effect.
- The diamond coating deteriorates the machinability more than the TiB2 coating. Diamond coating thickness leads to increase the cutting edge radius as well as the intrinsic friction response of the cutting tool by changing the tool surface morphology.
- Even if the diamond coating has the highest intrinsic friction response. The drilling friction induced by the diamond coated tool is the lowest. This is a consequence of the multiscale friction mechanisms that occur at the tool/composite interfaces and are due to the coating surface morphology.

References

[1] Dittenber DB, GangaRao HVS. Critical review of recent publications on use of natural composites in infrastructure. Compos Part A Appl Sci Manuf 2012;43:1419–29. https://doi.org/10.1016/j.compositesa.2011.11.019.

[2] Shalwan A, Yousif BF. In State of Art: mechanical and tribological behaviour of polymeric composites based on natural fibres. Mater Des 2013;48:14–24. https://doi.org/10.1016/j.matdes.2012.07.014.

[3] Shah DU. Developing plant fibre composites for structural applications by optimising composite parameters: a critical review. J Mater Sci 2013;48:6083–107. https://doi.org/10.1007/s10853-013-7458-7.

[4] Chegdani F, Mezghani S, El Mansori M, Mkaddem A. Fiber type effect on tribological behavior when cutting natural fiber reinforced plastics. Wear 2015;332–333:772–9. https://doi.org/10.1016/j.wear.2014.12.039.

[5] Chegdani F, Mezghani S, El Mansori M. Experimental study of coated tools effects in dry cutting of natural fiber reinforced plastics. Surf Coatings Technol 2015;284:264–72. https://doi.org/10.1016/j.surfcoat.2015.06.083.

[6] Chegdani F, Mezghani S, El Mansori M. On the multiscale tribological signatures of the tool helix angle in profile milling of woven flax fiber composites. Tribol Int 2016;100:132–40. https://doi.org/10.1016/j.triboint.2015.12.014.

[7] Chegdani F, Mezghani S, El Mansori M. Correlation between mechanical scales and analysis scales of topographic signals under milling process of natural fibre composites. J Compos Mater 2017;51:2743–56. https://doi.org/10.1177/0021998316676625.

[8] Babu GD, Babu KS, Gowd BUM. Effect of machining parameters on milled natural fiber-reinforced plastic composites. J Adv Mech Eng 2013:1–12. https://doi.org/10.7726/jame.2013.1001.

[9] Abdul Nasir AA, Azmi AI, Khalil ANM. Measurement and optimisation of residual tensile strength and delamination damage of drilled flax fibre reinforced composites. Measurement 2015;75:298–307. https://doi.org/10.1016/j.measurement.2015.07.046.

[10] Nassar MMA, Arunachalam R, Alzebdeh KI. Machinability of natural fiber reinforced composites: a review. Int J Adv Manuf Technol 2017;88:2985–3004. https://doi.org/10.1007/s00170-016-9010-9.

[11] Bajpai PK, Singh I. Drilling behavior of sisal fiber-reinforced polypropylene composite laminates. J Reinf Plast Compos 2013;32:1569–76. https://doi.org/10.1177/0731684413492866.

[12] Venkateshwaran N, ElayaPerumal A. Hole quality evaluation of natural fiber composite using image analysis technique. J Reinf Plast Compos 2013;32:1188–97. https://doi.org/10.1177/0731684413486847.

[13] Bajpai PK, Debnath K, Singh I. Hole making in natural fiber-reinforced polylactic acid laminates. J Thermoplast Compos Mater 2017;30:30–46. https://doi.org/10.1177/0892705715575094.

[14] Chegdani F, El Mansori M, Mezghani S, Montagne A. Scale effect on tribo-mechanical behavior of vegetal fibers in reinforced bio-composite materials. Compos Sci Technol 2017;150:87–94. https://doi.org/10.1016/j.compscitech.2017.07.012.

[15] Nosonovsky M, Bhushan B. Multiscale friction mechanisms and hierarchical surfaces in nano- and bio-tribology. Mater Sci Eng R Rep 2007;58:162–93. https://doi.org/10.1016/J.MSER.2007.09.001.

[16] Hocheng H. Machining technology for composite materials: principles and practice. Woodhead Pub; 2011.

[17] Mezghani S, El Mansori M, Sura E. Wear mechanism maps for the belt finishing of steel and cast iron. Wear 2009;267:86–91. https://doi.org/10.1016/j.wear.2008.12.113.

[18] Zacny KA, Cooper GA. Friction of drill bits under Martian pressure. J Geophys Res 2007;112, E03003. https://doi.org/10.1029/2005JE002538.

[19] Bhushan B. Introduction to tribology. Tridology. Wiley; 2013.

[20] Bowden FP, Tabor D. The friction and lubrication of solids. Oxf. Class. Clarendon Press; 2001.